

# Hidden Markov Model based Classification of Structural Damage

Wenfan Zhou<sup>a</sup>, Narayan Kovvali<sup>a</sup>, Antonia Papandreou-Suppappola<sup>a</sup>, Douglas Cochran<sup>a</sup>, and Aditi Chattopadhyay<sup>b</sup>

<sup>a</sup>Department of Electrical Engineering, Arizona State University, Tempe, AZ

<sup>b</sup>Department of Mechanical and Aerospace Engineering, Arizona State University, Tempe, AZ

## ABSTRACT

The ability to detect and classify damages in complex materials and structures is an important problem from both safety and economical perspectives. This paper develops a novel approach based on Hidden Markov Models (HMMs) for the classification of structural damage. Our approach here is based on using HMMs for modeling the time-frequency features extracted from time-varying structural data. Unlike conventional deterministic methods, the HMM is a stochastic approach which better accounts for the uncertainties encountered in the structural problem and leads to a more robust health monitoring system. The utility of the proposed approach is demonstrated via example results for the classification of fastener damage in an aluminum plate.

**Keywords:** structural health monitoring, damage detection, damage classification, matching pursuit decomposition, hidden Markov model

## 1. INTRODUCTION

The detection and classification of damage in complex materials and structures are important problems encountered in many applications. Existing techniques for dealing with these problems include those based on the use of non-destructive evaluation (NDE) techniques and time-frequency analysis,<sup>1</sup> wavelet transforms,<sup>2-4</sup> Lamb waves,<sup>5</sup> statistical pattern recognition techniques (based on time series analysis),<sup>6</sup> Bayesian networks,<sup>7</sup> and extreme value statistics.<sup>8</sup> Many of these methods, however, have drawbacks such as lack of robustness, limited sensitivity, and ultimately high cost, primarily because they fail to account for the uncertainties involved in the characterization of structural damage (for example, due to variability in structure geometry, material properties, measurement inaccuracy, and life history, and incomplete knowledge about the process of damage nucleation and evolution).

In this paper, we propose an algorithm for the classification of structural damage based on Hidden Markov Modeling (HMM) techniques.<sup>9,10</sup> The HMM is a powerful concept that is attractive not only owing to its rich mathematical structure but also because of its tremendous success in many other real-world applications, such as speech recognition,<sup>10</sup> target classification,<sup>11-13</sup> and image classification.<sup>14</sup> Unlike conventional deterministic methods, the HMM is a stochastic approach which better accounts for the uncertainties encountered in the structural problem. By aspiring to capture the statistical properties characterizing the underlying physical process, and by facilitating the integration of both available and unavailable information in a consistent manner, the HMM naturally leads to a more reliable and effective condition monitoring system.

Our approach here is based on using HMMs for the modeling of time-frequency damage features extracted from structural data. For the construction and validation of the models we rely on experimentally collected data. The first step is to extract features from the received signals and for this we employ the matching pursuit decomposition (MPD),<sup>15</sup> an algorithm known to be effective for the extraction of specific components of interest in a signal. Since the excitation used in our data is a linear frequency modulated chirp and the received signals have spectral characteristics which are strongly time-varying (the frequency content changes with time), we use MPD with a dictionary based on time-frequency Gabor atoms.<sup>15</sup> Given the MPD features of the time-varying received signals, the HMM defines underlying states (regions representative of the time-varying physical

---

Further author information: (Send correspondence to Narayan Kovvali)  
E-mail: Narayan.Kovvali@asu.edu, Telephone: 1 480 965 5954

states of the structure) and models the inter-state transitions and in-state observation statistics with a Markov random process. Note that the MPD features were quantized prior to the modeling because the HMMs utilized here are discrete observation-density HMMs.<sup>10</sup> Once built, the HMMs are integrated very efficiently into a Bayesian framework for the classification of structural damage. Results from an application to fastener damage classification demonstrate the utility of the proposed approach.

The remainder of this paper is organized as follows. Section 2 briefly discusses the MPD algorithm and Section 3 reviews the framework of HMMs. Section 4 describes the HMM-based structural damage classifier and presents an application for the classification of fastener damage in an aluminum plate. This is followed by conclusions in Section 5.

## 2. MATCHING PURSUIT DECOMPOSITION

The matching pursuit decomposition (MPD)<sup>15</sup> algorithm iteratively decomposes a given signal  $x(t)$  into a linear combination of normalized real basis functions or “atoms”  $\{g_i(t)\}_{i=0,\dots,K-1}$  as

$$x(t) = \sum_{i=0}^{K-1} \alpha_i g_i(t) + r_K(t), \quad (1)$$

where  $\alpha_i$  are the expansion coefficients, given by

$$\alpha_i = \int_{-\infty}^{\infty} r_i(t) g_i(t) dt, \quad i = 0, \dots, K - 1, \quad (2)$$

and  $r_i(t)$  denotes the residue function after the  $i$ -th decomposition (with  $r_o(t) \equiv x(t)$ ). The atoms are designed to *match* components of interest in the given signal class, and are chosen from a dictionary one-at-a-time in an iterative fashion so as to maximize the magnitude of the projections  $|\alpha_i|$  in (2) at each iteration. The dictionary is in general not an orthonormal set, but is required to be complete.<sup>15</sup>

The procedure ensures that the MPD yields the best-fit (in the sense of maximizing each single-step projection) most compact representation of the given signal in terms of the chosen family of basis functions. The truncation limit (number of expansion terms  $K$  in (1)) is usually chosen such that the energy of the residue after  $K$  iterations is smaller than some pre-defined value. If  $K$  is sufficient for the extraction of the most important signal components, the MPD by design effectively filters out unwanted signal components such as noise.

Good extraction of the discriminatory features between different signal classes is the critical first step for successful classification. In this paper, we make use of MPD with a dictionary composed of normalized time-frequency Gabor atoms<sup>15</sup> of the form

$$g_i(t) = e^{-\kappa_i^2 (t-\tau_i)^2} \cos(2\pi f_i t), \quad (3)$$

where  $\tau_i$  is time-shift,  $f_i$  frequency-shift, and  $\kappa_i$  scaling. These Gaussian-window harmonics have many advantages, including those derived from the availability of closed-form analytical expressions.<sup>15</sup>

## 3. HIDDEN MARKOV MODELING

In this section, we briefly review the framework of Hidden Markov Models (HMMs).<sup>9,10</sup>

The HMM is characterized by the set  $\lambda = \{\pi, A, B\}$ , where  $\pi$  is an  $N \times 1$  initial state distribution vector,  $A$  is an  $N \times N$  state transition probability distribution matrix, and  $B$  is an  $N \times M$  state-dependent observation symbol probability distribution matrix ( $N$  being the number of states, and  $M$  the number of distinct observation symbols in each state). The  $i$ th entry  $\pi_i$  of the vector  $\pi$  denotes the probability of state  $i$  at time  $t = 1$ , the  $(i, j)$ th entry  $a_{ij}$  of the matrix  $A$  denotes the probability of transitioning to state  $j$  at time  $t + 1$  from state  $i$  at time  $t$ , and the  $(j, k)$ th entry  $b_j(v_k)$  of the matrix  $B$  denotes the probability of observing symbol  $v_k$  when in state  $j$ . The HMM uses the parameters  $\pi$ ,  $A$ , and  $B$  to stochastically model finite-length sequences of observations. Specifically, given a finite-length observation sequence, the HMM defines underlying (non-observable or hidden)

regions of stationarity known as states and models the inter-state transitions and in-state observation statistics with a Markov random process. Note that here the observations are taken to be discrete symbols; such an HMM is known as a discrete HMM (because the state-dependent observation densities are discrete). The HMMs utilized in this work are discrete HMMs.

For the tasks of detection and classification, there are at least two basic problems of interest that must be solved. The first is to compute  $P(\mathbf{O}|\lambda)$ , the probability of an observation sequence  $\mathbf{O}$  given the model  $\lambda$ . The second is to adjust the model parameters  $\lambda = \{A, B, \pi\}$  to maximize  $P(\mathbf{O}|\lambda)$ . In the following, we outline the solutions to these problems (for more details see the tutorial by Rabiner<sup>10</sup>).

Let  $\mathbf{O} = O_1, O_2, \dots, O_T$  denote an observation sequence of length  $T$ , and  $Q = q_1, q_2, \dots, q_T$  the corresponding state sequence, with each  $q_t$  being one of  $N$  distinct states  $S_1, S_2, \dots, S_N$ . Assuming statistical independence of the observations symbols, the probability  $P(\mathbf{O}|Q, \lambda)$  of the observation sequence  $\mathbf{O}$ , given the model  $\lambda$  and a possible state sequence  $Q$ , can be expressed as

$$P(\mathbf{O}|Q, \lambda) = \prod_{i=1}^T P(O_i|q_i, \lambda) = b_{q_1}(O_1) \cdot b_{q_2}(O_2) \cdots b_{q_T}(O_T), \quad (4)$$

and the probability of the state sequence  $Q$ , given the model  $\lambda$ , is

$$P(Q|\lambda) = \pi_{q_1} \cdot a_{q_1 q_2} \cdots a_{q_{T-1} q_T}. \quad (5)$$

The joint probability of the observation sequence  $\mathbf{O}$  and the state sequence  $Q$ , given the model  $\lambda$ , is then

$$P(\mathbf{O}, Q|\lambda) = P(\mathbf{O}|Q, \lambda)P(Q|\lambda), \quad (6)$$

from which the probability of the observation sequence  $\mathbf{O}$ , given the model  $\lambda$ ,  $P(\mathbf{O}|\lambda)$  can be obtained as

$$P(\mathbf{O}|\lambda) = \sum_{\text{all } Q} P(\mathbf{O}, Q|\lambda) = \sum_{\text{all } Q} \pi_{q_1} \cdot b_{q_1}(O_1) \cdot a_{q_1 q_2} \cdot b_{q_2}(O_2) \cdots a_{q_{T-1} q_T} \cdot b_{q_T}(O_T). \quad (7)$$

Note that the direct computation of  $P(\mathbf{O}|\lambda)$  from (7) is very intensive (requires  $2T \times N^T$  operations). Fortunately, this computation can be carried out in a very efficient manner using the forward-backward procedure<sup>10</sup> (which reduces the computational complexity to  $N^2T$ ). Details can be found in.<sup>10</sup>

To find the model  $\lambda$  that leads to a (locally) maximized  $P(\mathbf{O}|\lambda)$ , a maximum-likelihood estimation process is realized through an expectation-maximization iterative reestimation procedure known as the Baum-Welch method.<sup>10</sup> In this algorithm, a previously estimated  $\lambda$  is iteratively replaced by a new estimate  $\hat{\lambda}$ . The new estimate  $\hat{\lambda}$  is provably better than or at least as good as the previous one in the sense that  $P(\mathbf{O}|\hat{\lambda}) \geq P(\mathbf{O}|\lambda)$ .<sup>10</sup> The reestimation is repeated to improve the probability until some limit point is achieved. Multiple observation sequences can be used to obtain a reliable estimate of the model parameters. Note that, in practice, a scaling procedure is applied to the algorithm to ensure that the implementation is numerically stable in finite-precision arithmetic (this issue arises because of the manipulation of a large number of products involving extremely small probabilities which can exceed the dynamic range of a computer's precision).

#### 4. APPLICATION OF HMM TO FASTENER DAMAGE CLASSIFICATION

In this section, we describe an application of the proposed HMM-based structural damage classifier for the classification of fastener damage in an aluminum plate.

##### 4.1. Experimental Setup and Data Collection

The data concerns fastener failure (loose bolt) experiments conducted at the Advanced Structural Concepts Branch, Air force Research Lab, with the test article being a four-bolt aluminum plate<sup>16</sup> (see Figure 1). The objective is to design a damage detection and localization system, with damage defined as a bolt being loose. This definition can be useful for many applications, for example, a loose-bolt could be indicative of a space vehicle's thermal protection system (TPS) about to come off.

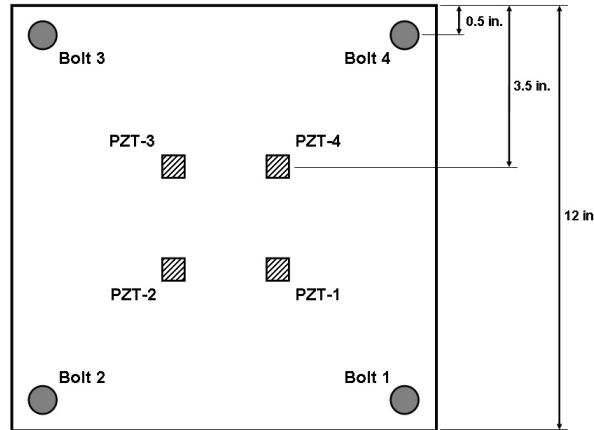


**Figure 1.** Schematic showing the experimental setup for fastener damage in a square aluminum plate.<sup>16</sup>

Data was collected in many rounds, and comprises the responses from three piezoelectric (PZT) sensors to a 0-1.5 kHz linear chirp excitation (all sampled at 5 kHz) for the five different structural conditions corresponding to one of the bolts being at 25% torque (30 inch-pound) or all bolts being at 100% torque (120 inch-pound). This gives rise to five different structural conditions (classes) for classification. Altogether, from each of the three receivers, we have 400 signals each for the first four structural conditions and 1,600 for the last. Figure 2 shows example plots of the signal transmitted by PZT-1 and the signals received by PZT-3 for the five classes.

## 4.2. Preprocessing, Feature Extraction, and Vector Quantization

The measured signals were first mean-centered, normalized, and time-aligned. Feature extraction was then performed using matching pursuit decomposition (MPD). For each waveform, the MPD was carried out to  $K = 60$  iterations with a dictionary composed of 42 million normalized time-frequency Gabor atoms. Figures 3(a)-3(c) show example plots of a preprocessed class 4 signal, the same signal after 60 iterations of MPD, and the residual signal energy versus MPD iteration number  $K$ . The residual energy decreases as  $K$  increases. Note that the choice  $K = 60$  corresponds to a residual energy of about 20%. The atoms in the MPD of each signal are fully characterized by the parameters  $\tau_i$ ,  $f_i$ ,  $\kappa_i$  (eq. (3)), and the expansion coefficients  $\alpha_i$  (eq. (2)), for  $i = 0, \dots, K - 1 = 59$ . The extracted atoms were then time-ordered, with the associated set of MPD parameters as the feature vectors, thus forming a length  $T = K = 60$  observation vectors to be modeled by an HMM.

Since the HMMs utilized in this work are *discrete* HMMs, the features had to be discretized prior to the modeling. This operation was carried out using vector quantization (VQ),<sup>17</sup> a nearest-neighbor classification process that maps each feature vector onto one of a finite set of symbols  $C = \{v_1, v_2, \dots, v_M\}$  referred to as the codebook. Here we determine the VQ codebook using the Linde-Buzo-Gray algorithm.<sup>17</sup> Note that the distance metric employed here for computing the “distortion” (quantization error) is the Mahalanobis square distance (MSD)<sup>17</sup>

$$d^2(\mathbf{x}_i, \mathbf{x}_j) = (\mathbf{x}_i - \mathbf{x}_j)^T \Lambda^{-1} (\mathbf{x}_i - \mathbf{x}_j), \quad (8)$$

where  $\mathbf{x}_i$  and  $\mathbf{x}_j$  are vectors,  $\Lambda = E[(\mathbf{x} - E[\mathbf{x}])(\mathbf{x} - E[\mathbf{x}])^T]$  is the covariance matrix, with  $E[\cdot]$  denoting the expected value. Figure 4 shows a plot of the average distortion as a function of the codebook size  $M$ . As expected, the distortion decreases as  $M$  increases. We use  $M = 400$  codes for quantization, corresponding to a distortion of about 0.025.

## 4.3. Hidden Markov Modeling and Choice of Model Parameters

As described in Section 3, the HMM is characterized by the set  $\lambda = \{\pi, A, B\}$  where  $\pi$  is the  $N \times 1$  initial state distribution vector,  $A$  is the  $N \times N$  state transition probability distribution matrix, and  $B$  is the  $N \times M$

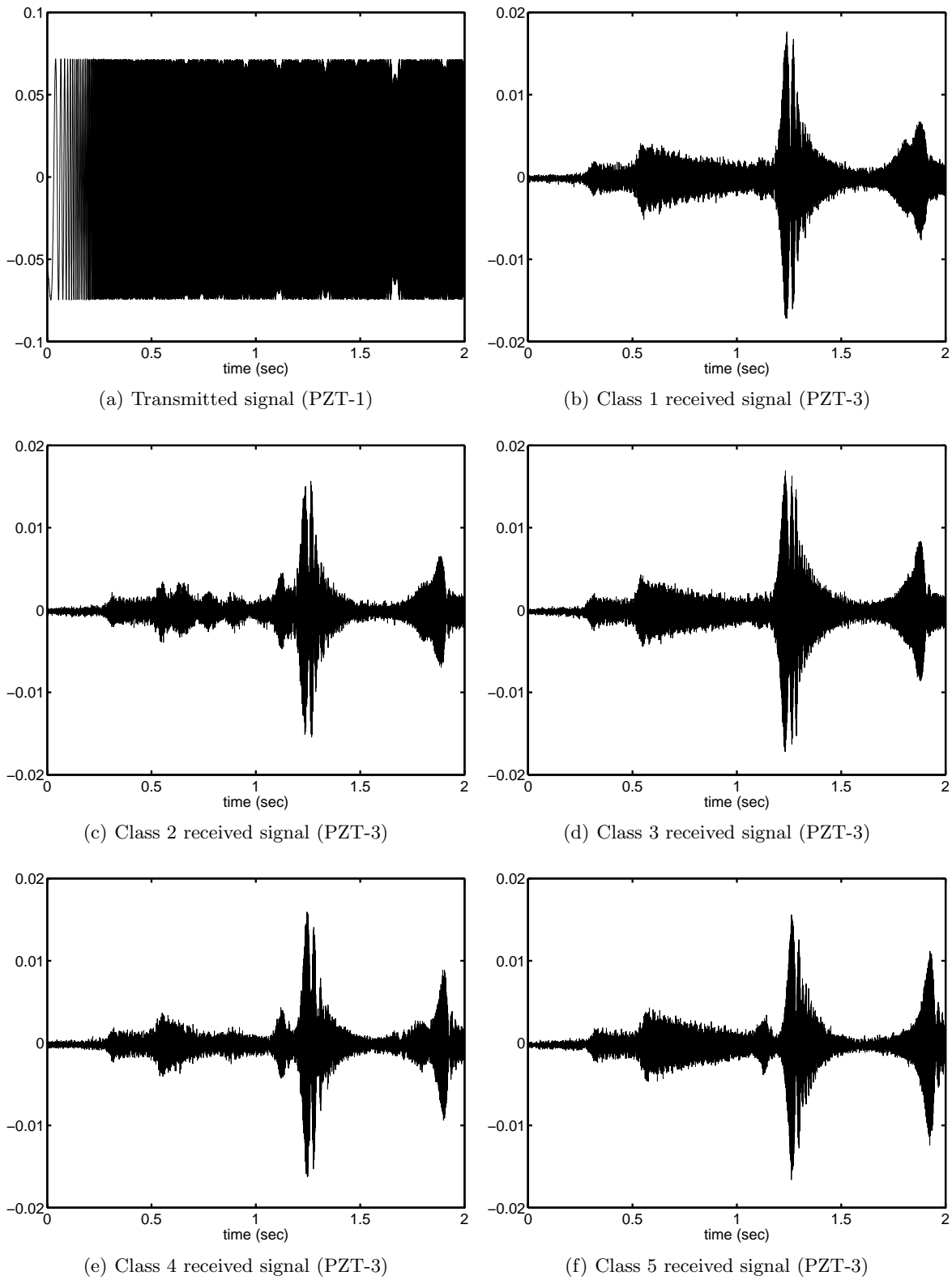


**Figure 2.** Example plots showing the signal transmitted by PZT-1 and the signals received by PZT-3 for the five classes.

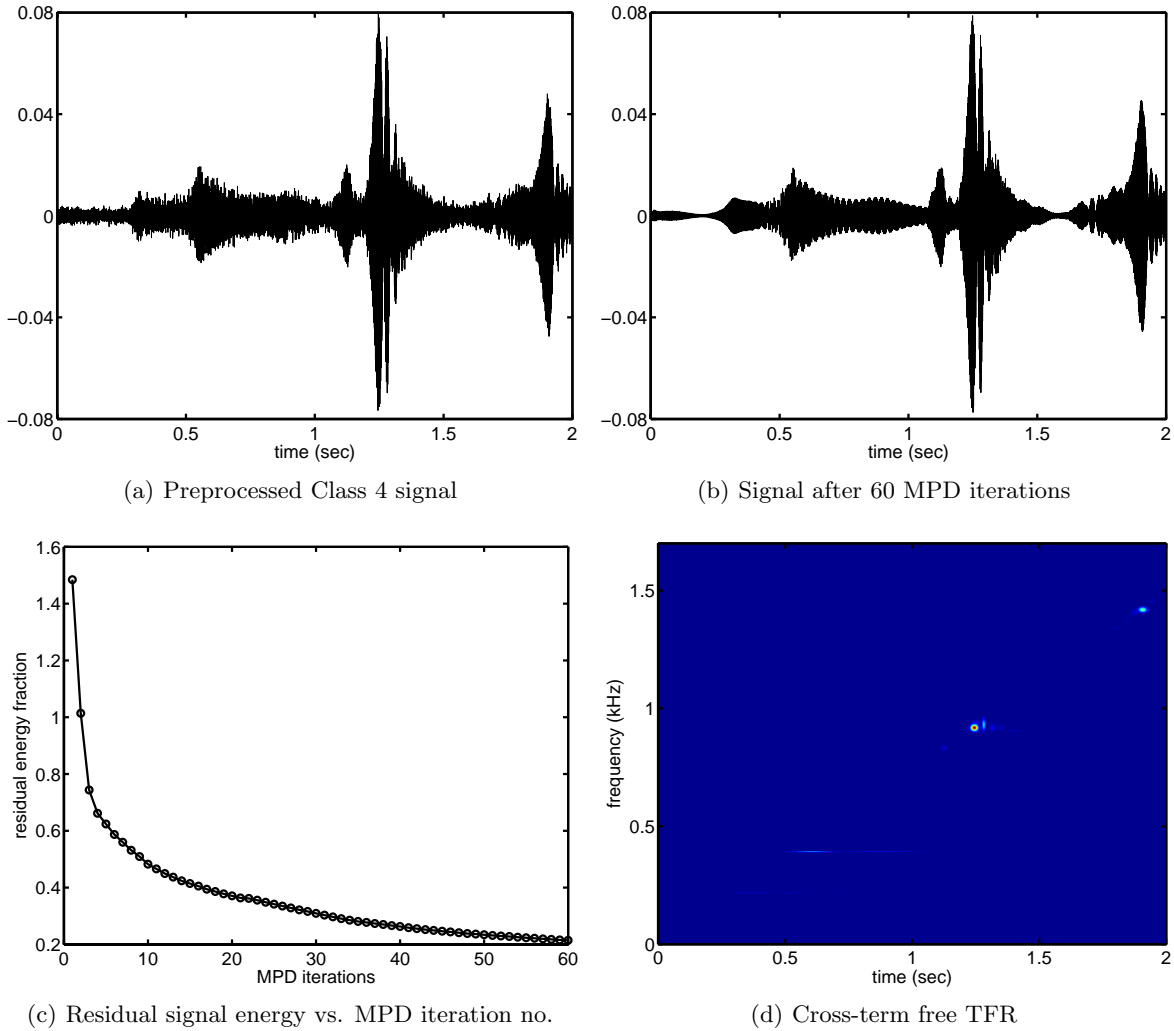


**Figure 3.** Example plots showing a preprocessed Class 4 signal, the same signal after 60 iterations of MPD, the residual signal energy versus MPD iteration number, and the corresponding cross-term free TFR.

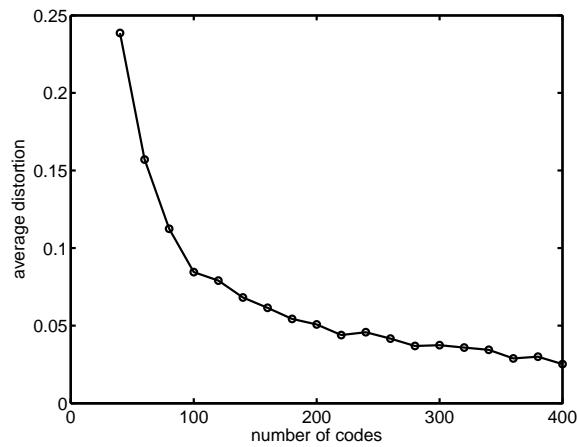


**Figure 4.** VQ distortion as a function of codebook size  $M$ .

state-dependent observation symbol probability distribution matrix ( $N$  being the number of states, and  $M$  the number of distinct observation symbols). In the present application, the states of the HMM correspond to the different physical states induced in the structure in response to the highly time-varying chirp excitation (different sets of resonant modes get excited as the actuator input sweeps the spectrum). The HMM works by modeling the temporal transitions between these underlying states in conjunction with the associated observation statistics. The data from each structural condition (class) is modeled with a separate HMM because the physics is different in each case (the variations in the bolt torque levels affect the boundary conditions on the plate, which in turn dictates what resonant modes get excited in response to the actuator input).

The number of states  $N$  is estimated by examining the time-frequency characteristics of the training data. For this purpose we make use of the cross-term free time-frequency representation (TFR)<sup>15</sup>

$$\mathcal{E}(t, f) = \sum_{i=0}^{K-1} |\alpha_i|^2 \text{WD}_{g_i}(t, f), \quad (9)$$

where WD denotes the Wigner distribution,<sup>18</sup> given for a signal  $x(t)$  by

$$\text{WD}_x(t, f) = \int_{-\infty}^{\infty} x\left(t + \frac{\tau}{2}\right) x^*\left(t - \frac{\tau}{2}\right) e^{-j2\pi f\tau} d\tau. \quad (10)$$

Note that the cross-term free TFR can be computed directly from the signal MPD. Note, furthermore, that it can be computed analytically because the Wigner distribution of the Gabor dictionary atoms  $g_i(t)$  are known in closed form.<sup>18</sup> Figure 3(d) shows the TFR for the example class 4 signal considered earlier. In our application,  $N$  is usually chosen to be around 3 or 4 depending on the class in question. Our simulations indicate that the performance of the classifier is not very sensitive to this choice. The expectation maximization (EM) algorithm which is used to train the HMMs is an iterative method that requires an initial guess for the model parameters  $\{\pi, A, B\}$ . These are determined using the state estimates above. Numerical experience shows that this approach yields a good initial guess, one that works much better than uniformly random values. The number of distinct observation symbols  $M$  has already been taken as  $M = 400$  (the size of the codebook used for quantization), which completes the choice of model parameters.

#### 4.4. Classification Results

Half of the data set was used for training the HMMs (estimating model parameters) and half for testing the classifier performance. Figure 5 shows a plot of the (class 1) data log-likelihood versus training iteration number. The log-likelihood increases monotonically with the training iterations. In our simulations, we found that about 10 to 20 iterations are usually sufficient for convergence of the likelihood. Once trained, the HMMs are integrated very efficiently into a Bayesian framework for the classification of structural damage. Observations are classified based on their likelihood as computed from the HMM associated with each class. Specifically, the classifier assigns a given test observation  $\mathbf{O}$  to class  $k$  such that

$$k = \underset{j}{\operatorname{argmax}} P(\mathbf{O}|\lambda_j), \quad (11)$$

where  $\lambda_j$  denotes the  $j$ th HMM (trained on data from class  $j$ ).

The performance of the classifier is quantified here by means of a  $5 \times 5$  confusion matrix. Essentially, the  $(i, j)$ th element of this matrix indicates the probability that data from class  $i$  is classified as being from class  $j$ . Ideally, this would be a  $5 \times 5$  identity matrix. For our HMM-based structural damage classifier, we obtain the confusion matrix:

$$\begin{bmatrix} 0.80500 & 0.05500 & 0.13500 & 0 & 0.00500 \\ 0 & 0.98000 & 0.00500 & 0 & 0.01500 \\ 0.05500 & 0.08000 & 0.86500 & 0 & 0 \\ 0.00500 & 0.02000 & 0 & 0.97000 & 0.00500 \\ 0 & 0 & 0 & 0.00125 & 0.99875 \end{bmatrix}. \quad (12)$$

We find that the performance of the HMM-based classifier is high (the average percentage correct classification is above 90%), demonstrating the utility of this approach.

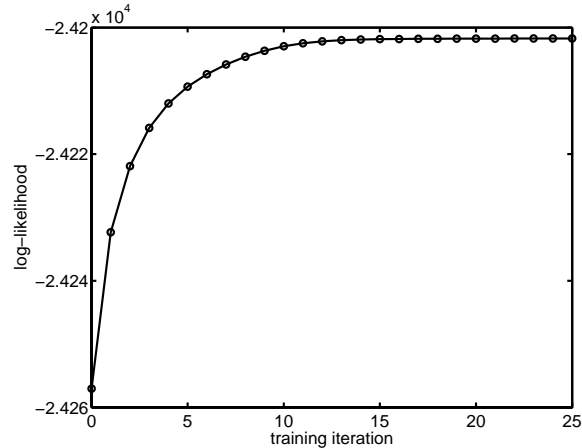


Figure 5. Class 1 data log-likelihood versus HMM training iteration number.

## 5. CONCLUSION

In this paper, we have presented a novel HMM-based algorithm for the classification of structural damage. Application to fastener damage in an aluminum plate shows that the performance of the HMM-based damage classifier is very good, with percentage correct classification near 90%. This is an encouraging result, and yet there are many ways in which the performance can be improved further. Firstly, note that the time-frequency MPD dictionary employed here is based on Gabor atoms and  $K = 60$  MPD iterations are needed to bring the residual energy to about 20%. We are currently investigating a dictionary that uses chirps instead of Gabor functions. The idea is that such a dictionary is better-matched to the signals of interest here and consequently the error is expected to be smaller with fewer iterations, leading to savings in computational costs. Second, since the HMMs utilized in this work are discrete HMMs, the MPD features had to be discretized prior to the modeling. This quantization process obviously results in added artifacts which affect classifier performance in an adverse manner. In our latest implementations, we are therefore incorporating *continuous* HMMs<sup>10</sup> based on Gaussian mixture model observation densities where the data being modeled is not restricted to be discrete. This completely eliminates the quantization step and its associated errors, thereby boosting the algorithm's performance. In addition, for simplicity, only data collected from PZT-3 was used in our present simulations. However, in order to have optimal classification performance, the data obtained from the other sensors (PZT-2 and PZT-4) must also be utilized. As a next step, we plan to address the fusion of information from the sensors. All this forms the subject of current research and results will be reported at a future date.

## ACKNOWLEDGMENTS

This research was supported by the Department of Defense AFOSR Grant FA95550-06-1-0309 (Program manager: Victor Giurgiutiu). The authors would like to thank M. Derriso, M. DeSimio, and S. Olson (AFRL, Wright Patterson AFB) for providing the experimental data used in this paper.

## REFERENCES

1. W. J. Staszewski, C. Boller, and G. R. Tomlinson, *Health Monitoring of Aerospace Structures*, Wiley, England, 2003.
2. H. Jeong and Y.-S. Jang, "Fracture source location in thin plates using the wavelet transform of dispersive waves," *IEEE Transactions on Ultrasonics, Ferroelectrics, and Frequency Control* **47-3**, pp. 612–619, 2000.
3. L. Eren and M. J. Devaney, "Bearing damage detection via wavelet packet decomposition of the stator current," *IEEE Transactions on Instrumentation and Measurement* **53-2**, pp. 431–436, 2004.
4. A. Sun and C. C. Chang, "Statistical wavelet-based method for structural health monitoring," *Journal of structural engineering*, pp. 1055–1062, 2004.

5. V. Giurgiutiu, "Tuned Lamb wave excitation and detection with piezoelectric wafer active sensors for structural health monitoring," *Journal of Intelligent Material Systems and Structures* **16**, pp. 291–305, 2005.
6. H. Sohn, C. R. Farrar, N. F. Hunter, and K. Worden, "Structural health monitoring using statistical pattern recognition techniques," *Transactions of the ASME* **123**, pp. 706–711, 2001.
7. M. Nguyen, X. Wang, Z. Su, and L. Ye, "Damage identification for composite structures with a Bayesian network," *ISSNIP* , pp. 307–312, 2004.
8. H. Sohn, D. W. Allen, K. Worden, and C. R. Farrar, "Structural damage classification using extreme value statistics," *Journal of Dynamic Systems, Measurement, and Control* **127**, pp. 125–132, 2005.
9. L. R. Rabiner and B. H. Juang, "An introduction to hidden Markov models," *IEEE ASSP Magazine* , pp. 4–15, 1986.
10. L. R. Rabiner, "A tutorial on hidden Markov models and selected applications in speech recognition," *Proceedings of the IEEE* **77**, pp. 257–286, 1989.
11. P. R. Runkle, P. K. Bharadwaj, L. Couchman, and L. Carin, "Hidden Markov models for multispect target classification," *IEEE Transactions on Signal Processing* **47**, pp. 2035–2040, 1999.
12. P. K. Bharadwaj, P. Runkle, and L. Carin, "Target identification with wave-based matched pursuits and hidden Markov models," *IEEE Transactions on Antennas and Propagation* **47**, pp. 1543–1554, 1999.
13. P. Runkle, L. Carin, L. Couchman, T. J. Yoder, and J. A. Bucaro, "Multiaspect target identification with wave-based matched pursuits and continuous hidden Markov models," *IEEE Transactions on Pattern Analysis and Machine Intelligence* **21**, pp. 1371–1378, 1999.
14. J. Li, A. Najmi, and R. M. Gray, "Image classification by a two dimensional hidden Markov model," *IEEE Transactions on Signal Processing* **48**, pp. 517–533, 2000.
15. S. G. Mallet and Z. Zhang, "Matching pursuits with time-frequency dictionaries," *IEEE Transactions on Signal Processing* **41**, pp. 3397–3415, 1993.
16. S. E. Olson, M. P. DeSimio, and M. M. Derriso, "Fastener damage estimation in a square aluminum plate," *Structural Health Monitoring* **5**, pp. 173–183, 2006.
17. Y. Linde, A. Buzo, and R. M. Gray, "An algorithm for vector quantizer design," *IEEE Transactions on Communications* **COM-28**, pp. 84–95, 1980.
18. A. Papandreou-Suppappola, ed., *Applications in Time-Frequency Signal Processing*, CRC Press, Florida, 2002.